

Geoelectric Evaluation of Aquifer Potential and Vulnerability of Northern Paiko, Niger State, Nigeria

Daniel N. Obiora^{1*}, Usman D. Alhassan², Johnson C. Ibuot¹, Francisca N. Okeke¹

ABSTRACT: This study was carried out using vertical electrical sounding (VES) to evaluate the groundwater potential and the aquifer protective capacity of Northern Paiko. Sixty vertical electrical soundings were obtained across the study area using Schlumberger electrode configuration. Three to four geoelectric layers were delineated from the interpreted results. The stratigraphy of the subsurface shows: topsoil (62.8–3082 Ωm), weathered layer (15.2–80 368 Ωm), fractured layer (191–236 672 Ωm), and the fresh basement (79.9–308 865 Ωm). The weathered layer was delineated as the major aquiferous horizon. From the results, the resistivity, thickness, and longitudinal conductance maps were drawn. It was observed that groundwater potential is low in about 76.7% of the study area. This study has also shown that the aquifer protective capacity of most parts of the study area is poor (83.3%), thus rendering the aquifer vulnerable to contamination. *Water Environ. Res.*, **88**, 644 (2016).

KEYWORDS: geoelectric layers, Northern Paiko, aquifer potential, longitudinal conductance, Schlumberger configuration, aquifer protective capacity.

doi:10.2175/106143016X14609975746569

Introduction

The knowledge of groundwater potential of an area is essential for sustainable groundwater development. To meet the water needs of the ever-growing population and urbanization of Paiko, groundwater is in high demand. The inadequacy of municipal water has led to overdependence on groundwater from hand-dug wells or borehole systems by individuals to complement the public or municipal water supply. Groundwater has a natural protection against pollution by the covering layer and requires minor water treatment. The basement complex has many challenges as regards to groundwater potential evaluation (Olasehinde and Amadi, 2009) and it explains why well yield in the basement complex is lower than well yield in sedimentary terrain (Adeleye, 1976; Amadi et al., 2010). Protection of groundwater against pollution is very important because the quality of groundwater is under threat of potential contamination resulting from leaching of contaminants to groundwater.

Consumption of polluted water has a serious health implication that made the quality of groundwater exploited for drinking and domestic uses the authors' major concern. To address the hydrological and hydrogeological problems, there is need to quantitatively describe the groundwater repositories by considering properties such as resistivity, thickness, and longitudinal conductance. The combination of layer resistivity and thickness in Dar Zarruk parameters S (longitudinal conductance) and T (transverse resistance) may be of direct use in aquifer protection studies. Factors that affect groundwater contamination are permeability, porosity, and overburden thickness of geologic formation.

The electrical resistivity method (noninvasive) has been used successfully by several researchers and authors for groundwater investigation (Abiola et al., 2009; Barker et al., 2001; George et al., 2010; Lashkaripour, 2003; Niwas and Singhal, 1981; Singh, 2005). This method is preferable because of the resistivity contrasts obtained when the groundwater zone is reached. In the basement area, several authors have researched groundwater exploration, evaluation, and delineation using geophysical methods (Adeniji et al., 2013; Dan-Hassan, 2001; Egbai, 2011). The electrical resistivity contrasts between lithological sequences in the subsurface are often adequate to enable the delineation of geoelectric layers and identification of aquiferous or non-aquiferous layers. Water from the basement complex contains calcium or sodium bicarbonate, nitrate in high concentration of health implication (Du preez and Barber, 1965). Groundwater usually occurs in discontinuous aquifers in basement complex areas. The highest groundwater yield in basement terrains is found in areas where thick overburden overlies fractured zones. These zones are often characterized by relatively low resistivity values (Olurunfemi and Fasuyi, 1993). The indiscriminate sinking of boreholes without preliminary geological, geophysical and hydrogeological investigation has resulted in some boreholes being drawn or abandoned. The efforts of government and nongovernmental organizations in making safe drinking water available have been successful in some communities. Resulting from uncoordinated drilling, some boreholes and hand-dug wells have poor yield in the dry season when rainfall stops.

The aim of this study is to evaluate the groundwater potential of northern Paiko and to establish the aquifer protective capacity of the overlying layer. It is believed that the result of this study will be useful in assessing and managing groundwater repositories of the area.

¹ Department of Physics and Astronomy, University of Nigeria, Nsukka, Nigeria.

² Department of Physics, Federal University of Technology, Minna, Nigeria.

* Department of Physics and Astronomy, University of Nigeria, Nsukka, Nigeria; e-mail: daniel.obiora@unn.edu.ng.

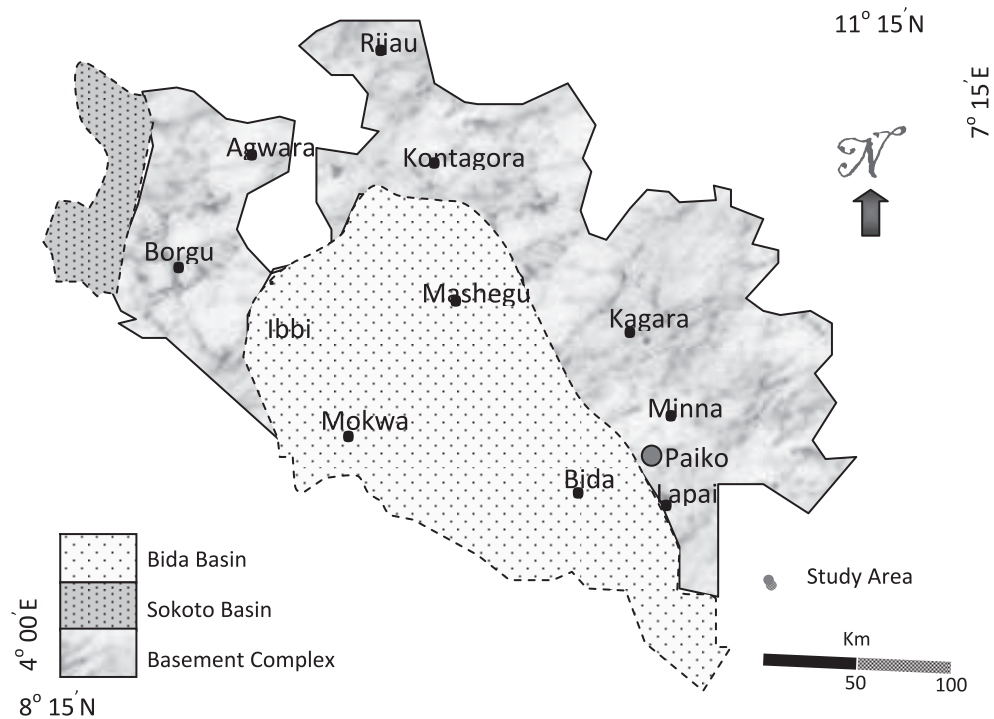


Figure 1—Geological map of Niger State basement complex and sedimentary basins (Amadi et al., 2012).

Location and Geology of the Study Area

The study area, Paiko, is located in Niger State, in the north-central part of Nigeria. It lies within latitudes 9°25'N and 9°27'N, longitudes 6°37'E and 6°39'E, with an elevation of 304 m above sea level. The vegetation in the area is of the Guinea savanna type, which is characterized by annual rainfall variation of 1200–

1300 mm. The mean annual temperature is between 22 to 25 °C. The Kaduna River and its tributaries drain the area. The topography is fairly undulating with expanses of plain lands in the eastern part of the study area, while the western part is characterized by very high steep-sided hills. Paiko Hill is the highest hill in the vicinity with an elevation of 60 m. The study



Figure 2—Google Earth map showing VES stations.

Table 1—Summary of measured geoelectric parameters in the study area.

Long/deg	Lat/deg	VES station	No. of layers	ρ_1 (Ωm)	ρ_2 (Ωm)	ρ_3 (Ωm)	ρ_4 (Ωm)	h_1 (m)	h_2 (m)	h_3 (m)	h_4 (m)	Curve type	Longitudinal conductance S (Ω^{-1})
6.65329	9.33721	G ₁	3	1248	184	60671		1.4	4.6	∞		H	0.025
6.65361	9.33695	G ₂	3	1720	526	11221		1.38	5.89	∞		H	0.011
6.65445	9.33655	G ₃	3	667	126	12178		1.15	2.92	∞		H	0.0233
6.65403	9.33677	G ₄	3	947	70.8	78315		1.63	3.47	∞		H	0.049
6.65476	9.33626	G ₅	4	820	247	1021	308865	1.04	0.85	24.4	∞	HA	0.024
6.65515	9.33599	G ₆	3	380	8244	1522		2.07	2.04	∞		K	0.0003
6.65544	9.33565	G ₇	3	1120	132	4920		2.07	1.06	∞		H	0.0083
6.65567	9.33531	G ₈	3	419	968	15552		3.91	19.4	∞		A	0.020
6.656	9.33497	G ₉	3	229	11184	1303		2.11	4.75	∞		K	0.0004
6.65636	9.33474	G ₁₀	3	117	351	13298		1.19	7.88	∞		A	0.023
6.65521	9.33774	H ₁	4	1490	152	750	117922	1.18	2.03	22.1	∞	HA	0.030
6.65563	9.33762	H ₂	3	415	124	3204		1.69	2.24	∞		H	0.018
6.65604	9.33746	H ₃	3	308	130	13859		1.42	1.86	∞		H	0.014
6.65604	9.33746	H ₄	3	1114	136	41263		1.93	5.23	∞		H	0.039
6.65604	9.33746	H ₅	3	39.9	60825	5239		3.07	72	∞		K	0.001
6.65648	9.3374	H ₆	3	1070	80368	224		1.38	3.43	∞		K	0.00004
6.65691	9.33718	H ₇	3	243	941	92291		1.05	24.3	∞		A	0.026
6.65732	9.33693	H ₈	3	457	700	215028		1.45	10.9	∞		A	0.016
6.65769	9.33668	H ₉	3	550	28	4233		1.12	2.17	∞		H	0.078S
6.65801	9.33643	H ₁₀	4	191	106	263	278439	1.43	1.6	14.6	∞	HA	0.056
6.65432	9.33803	I ₁	3	595	46.4	194453		1.37	1.96	∞		H	0.042
6.65478	9.33787	I ₂	3	761	110	3542		1.25	2.86	∞		H	0.026
6.65152	9.33661	I ₃	3	536	153	7580		1.52	3.23	∞		H	0.021
6.65173	9.33619	I ₄	3	527	32	103681		1.16	4.31	∞		H	0.135
6.65198	9.33581	I ₅	3	180	27.7	55673		1.22	4.02	∞		H	0.145
6.65224	9.33549	I ₆	3	1606	154	1796		1.12	2.6	∞		H	0.016
6.65256	9.33519	I ₇	3	764	34.1	2027		1.06	1.12	∞		H	0.033
6.6528	9.33479	I ₈	3	3082	131	43827		2.15	6.06	∞		H	0.046
6.65307	9.33441	I ₉	3	474	27	38527		1.61	2.36	∞		H	0.087
6.65338	9.33412	I ₁₀	3	1463	10.9	19302		1.11	1.67	∞		H	0.153
6.63792	6.63792	J ₁	3	841	223	2867		1.36	2.25	∞		H	0.010
6.63748	6.63748	J ₂	4	439	85.2	236672	696	1.35	2.18	5.04	∞	HK	0.00002
6.63704	6.63704	J ₃	3	1423	978	9225		8.53	7.2	∞		H	0.007
6.63704	6.63704	J ₄	4	985	189	94441	288	1.05	2.22	7.93	∞	HK	0.00008
6.63659	6.63659	J ₅	3	83.8	29.4	131987		1.86	3.99	∞		H	0.136
6.63615	6.63615	J ₆	2	62.2	1623			1.56	∞			A	0.025
6.63569	6.63569	J ₇	3	982	199	2950		0.95	2.59	∞		H	0.013
6.63523	6.63523	J ₈	4	387	140	398	118946	1.86	4.22	30.5	∞	HA	0.218
6.63477	6.63477	J ₉	3	620	11.2	58241		1	2	∞		H	0.179
6.63435	6.63435	J ₁₀	4	571	124	354	213414	1.3	1.43	15.1	∞	HA	0.043
6.63619	9.46551	K ₁	4	554	4846	296	196873	3.57	3.61	9.22	∞	KH	0.031
6.63751	9.46551	K ₂	3	636	978	5752		4.06	22.1	∞		A	0.023
6.63705	9.4655	K ₃	3	517	78	5437		1.17	2.05	∞		H	0.026
6.63661	9.46552	K ₄	3	178	111	6005		1.42	3.05	∞		H	0.028
6.63614	9.4655	K ₅	4	469	117	191	134745	1.07	1.93	12.7	∞	HA	0.0001
6.63486	9.4655	K ₆	3	198	331	95088		1.3	13.9	∞		A	0.042
6.63397	9.46549	K ₇	4	776	61.3	1478	59411	1.21	1.54	37.5	∞	HA	0.025
6.63309	9.46549	K ₈	3	712	61.2	108026		1.06	6.39	∞		H	0.104
6.6357	9.46548	K ₉	3	786	114	29362		2.02	14.1	∞		H	0.124
6.63525	9.4655	K ₁₀	3	433	113	1038		2.02	1.6	∞		H	0.014
6.63435	9.46549	L ₁	4	300	196	27962	79.9	2.69	5.23	7.41	∞	HK	0.0003
6.63353	9.46548	L ₂	4	620	154	38600	130	1.18	2.06	4.78	∞	HK	0.0001
6.63309	9.46547	L ₃	4	625	132	113317	303	1.28	1.75	3.75	∞	HK	0.00003
6.63792	9.46467	L ₄	3	1052	232	172184		1.24	11.4	∞		H	0.049
6.63703	9.46468	L ₅	3	656	289	4230		1.49	12.1	∞		H	0.042
6.63661	9.46467	L ₆	3	85	15.2	78682		1.13	4.13	∞		H	0.272
6.63573	9.46468	L ₇	3	584	156	2853		1.18	2.55	∞		H	0.016
6.63527	9.46468	L ₈	3	1003	59.8	31877		2.54	4.75	∞		H	0.079
6.63439	9.46468	L ₉	3	546	43.2	107599		1.42	6.12	∞		H	0.1412
6.63701	9.46467	L ₁₀	3	420	170	110943		2.31	12.1	∞		H	0.071

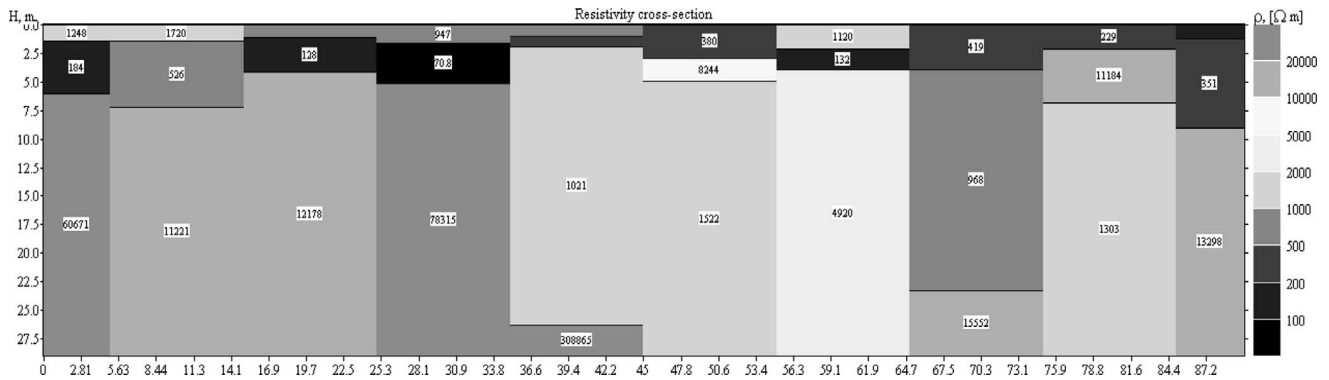


Figure 3—Profile showing the geoelectric section G.

area falls within the basement complex of Nigeria (Figure 1) and is underlain by four lithological formations as is evident from the rocks in the area. The rock types in this region include granites, gneisses, quartzite, as well as laterites. Most of the granites belong to the granite suites and this distinguishes them from the younger granites found in the Jos area. The mapped area is underlain by coarse to medium-grained granite, and the rocks are well exposed at the northern part of Paiko.

About half of the landmass of Niger State is underlain by the basement complex rocks, while the remaining half is occupied by Cretaceous sedimentary rocks of Bida Basin (Amadi et al., 2012). The main lateritic rock, which occurred in all parts of the area are of two forms: the first is dark brown, hard, and spongy in appearance, while the second is light brown, soft, and less spongy and is the oldest (Ajibade, 1980).

Data Acquisition and Interpretation

The ABEM SAS 4000 Terrameter was used for data acquisition to delineate the resistivity of the subsurface materials. The Schlumberger electrode configuration was used for each vertical electrical sounding (VES) station because of its sensitivity to surface inhomogeneities (Sharma, 1997). A total of 60 VES (Figure 2) were carried out in the study area with a maximum current electrode spacing ($AB/2$) of 100 m and maximum potential electrode spacing ($MN/2$) of 15 m. The measured apparent resistance R_a was converted to apparent resistivity ρ_a using eq 1:

$$\rho_a = \pi \left[\frac{\left(\frac{AB}{2}\right)^2 - \left(\frac{MN}{2}\right)^2}{MN} \right] R_a \tag{1}$$

where AB is the distance between the two current electrodes, MN is the distance between the potential electrodes, and R_a is the apparent electrical resistance measured from the equipment. Equation 1 can be simplified to

$$\rho_a = K \cdot R_a \tag{2}$$

where K is the geometric factor:

$$K = \pi \cdot \left[\frac{\left(\frac{AB}{2}\right)^2 - \left(\frac{MN}{2}\right)^2}{MN} \right]$$

A bi-logarithm graph was used to plot the computed apparent resistivity manually and the curves generated were smoothed to remove the effects of lateral inhomogeneities. The smoothed curves were quantitatively interpreted in terms of true resistivity and thickness by a conventional manual curve matching procedure using master curves and auxiliary charts (Orellana and Mooney, 1966).

The manually interpreted data were improved upon using Resist software, which produces geological curve models from the field data. The method of iteration was carried out until the fitting errors between the field data and theoretical curve fell below 10%. From the interpreted data, longitudinal conductance

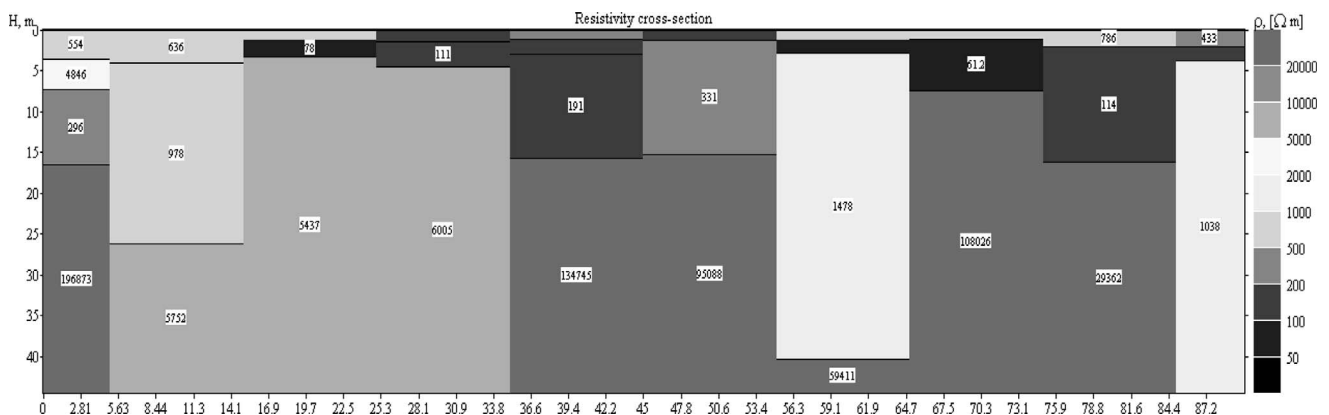


Figure 4—Profile showing the geoelectric section of K.

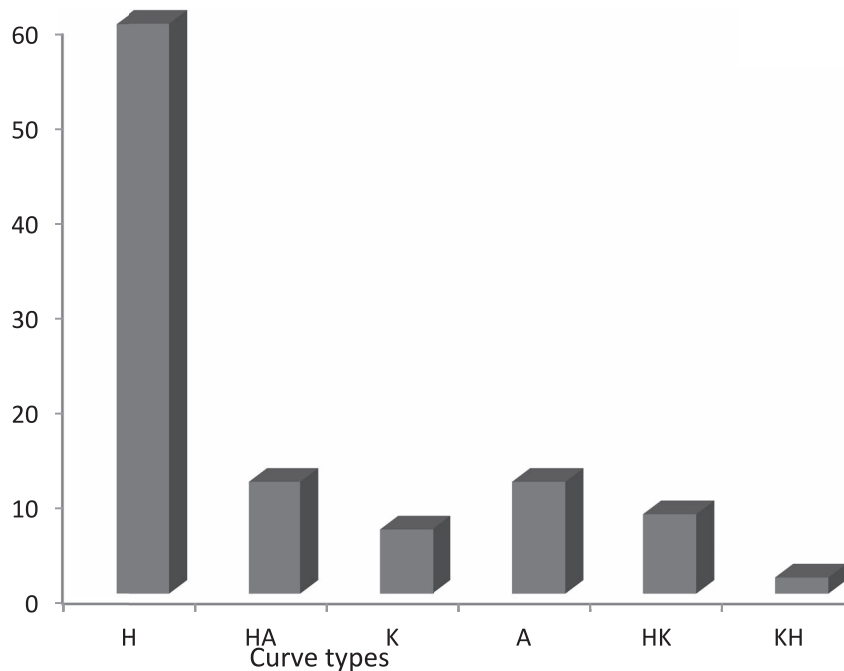


Figure 5—Bar chart showing frequency distribution in the study area.

(S) of the overburden layer at each VES station was obtained using

$$S = \sum_{i=1}^n \frac{h_i}{\rho_i} \quad (3)$$

where h_i is the saturated thickness of each layer and ρ_i is the true resistivity of each layer.

Results and Discussion

The results obtained from resistivity data interpretation is presented in Table 1. The geoelectric sections (Figures 3 and 4) were also generated from the data. The geoelectric sections reveal three to four geoelectric layers across the study area. The topmost layer with a resistivity range of 62.8–3082 Ωm was identified as topsoil and a thickness range of 0.95–8.57 m. This layer can be said to be dominated by moist to dry sand and gravel. The first layer is underlain with a weathered layer with resistivity ranging from 15.2–80 368 Ωm . The thickness of this layer ranges from 0.85–19.4 m. This layer is relatively thick and is a sandy unit as a result of weathering, thus the layer is highly porous and permeable and is observed to harbor approximately 76.7% of the aquifer in the study area. The third layer, whose thickness was not identified within the maximum current electrode separation in most of the VES station, was identified as weathered/fractured layer with a resistivity range of 191–236 672 Ωm . This layer is observed in some VES stations to be generally thick and 21.7% of the aquifer is found in this layer. The high resistivity values in Layer 3 shows the layer to be highly granitic. The fourth layer identified as fresh basement underlain the fractured layer and has a resistivity range of 79.9–308 865 Ωm . The thickness of this layer is generally not identified within the maximum current electrode separation. The relatively high resistivity values in Layer 3 indicates that the layer is made up of low conducting materials compared to Layers 1 and 2. The

frequency of curve distribution is shown Figure 5. The dominant curve type is H with 60.0%, which is characterized by VES with three layers, 11.7% of HA and A curve types, 8.3% of HK, 17.0% of KH, and 6.7% of K curve type.

The resistivity contour map of the study area (Figure 6) shows the variation of aquifer resistivity in the study area. High resistivity was observed in the extreme northeast of the study area, which is evidence for the presence of dense granite and sandstone. The greater portion of the study area from the north southward shows relatively low resistivity values with the least obtainable in the southeast and southwestern part of the study area. The distribution of aquifer thickness is shown in Figure 7. The whole of the northwestern and southwestern part show very low thickness while part of the north-central and northeastern parts have the highest depth in the study area. The greater part of the study area from the north down to the south has low aquifer thickness. The thickness and the nature of the weathered layer are important parameters in the groundwater potential evaluation of the basement complex terrain (Bala and Ike, 2001; Clerk, 1985). The groundwater potential of the study area shows high, medium, and low potentials. From this study, VES J_8 and K_7 with aquifer thickness greater than 25 m were considered as zones having high groundwater potential. This forms approximately 3.3% of the study area and is found in the north-central and in the northwest areas. This zone is likely to have high clay content. The medium groundwater potential zone with aquifer thickness ranging from 10–25 m is made up of 20% of the study area and the clay content there may be moderate. Of the study area, 76.7% has low groundwater potential with aquifer thickness below 10 m. The northwest down to the southwest has the lowest groundwater potential. The VES lithology of VES G_5 and VES H_{10} are corroborated with the lithological logs from nearby boreholes as shown in Figure 8.

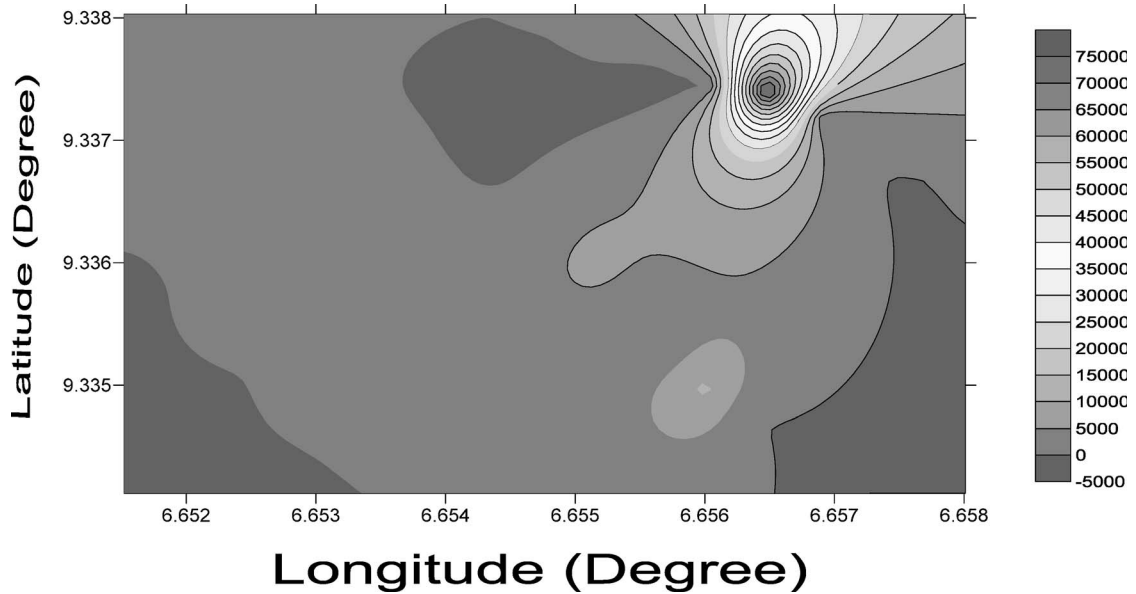


Figure 6—Contour map of aquifer resistivity in the study area.

A detailed distribution pattern of the natural overburden protection of the aquifer in the study area was obtained from the 2-D contour map (Figure 9). This was evaluated using the longitudinal conductance obtained from eq 3. The values of longitudinal conductance are used because the earth acts as a natural filter to the percolating fluid. The longitudinal conductance was used in accordance with the protective capacity rating of Table 2. This enables the classification of the study area into poor, weak, and moderate protective capacity zones. From Table 1, the longitudinal conductance

ranges from 0.272–0.00008 mhos. Of the study area, 83.3% has poor aquifer protective capacity with longitudinal conductance value of <0.1 mhos, 13.3% is weakly protected with values between 0.1 and 0.19 mhos, while 3.3% is moderately protected within the longitudinal conductance range of 0.2–0.69 mhos. The contour map clearly shows high longitudinal conductance in the southwestern part of the study area. The north-central part has very low longitudinal conductance, as such is poorly protected and vulnerable to contamination.

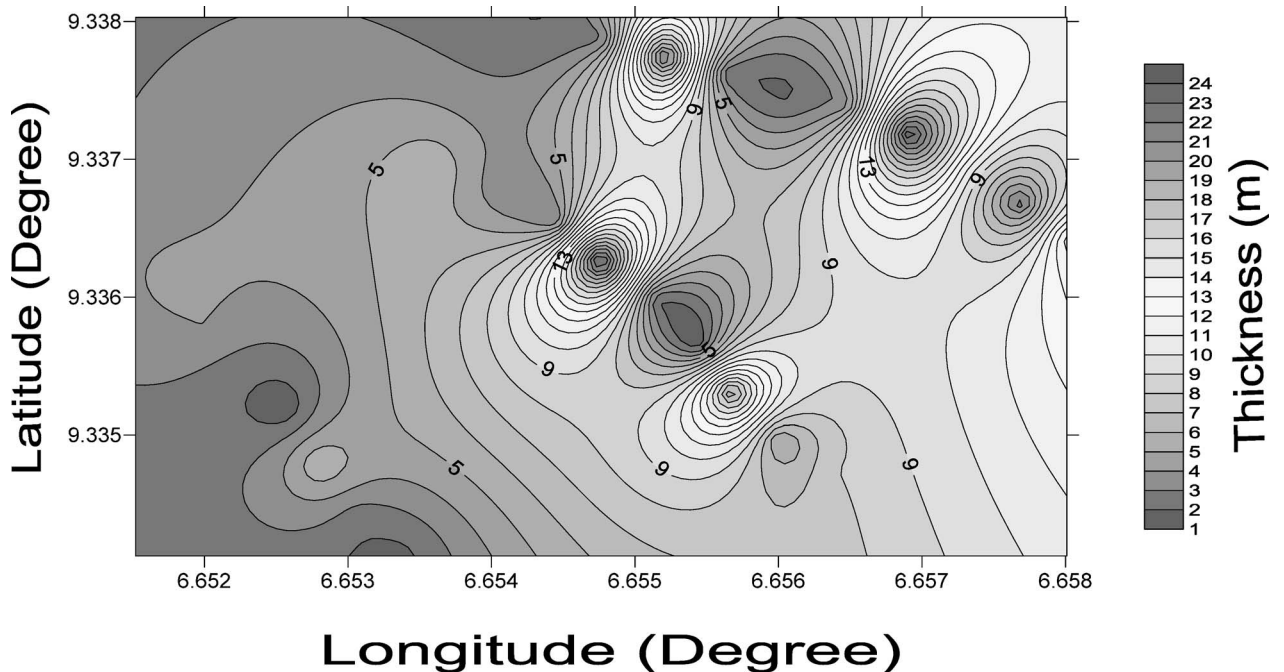


Figure 7—2-D contour map showing aquifer thickness distribution in the study area.

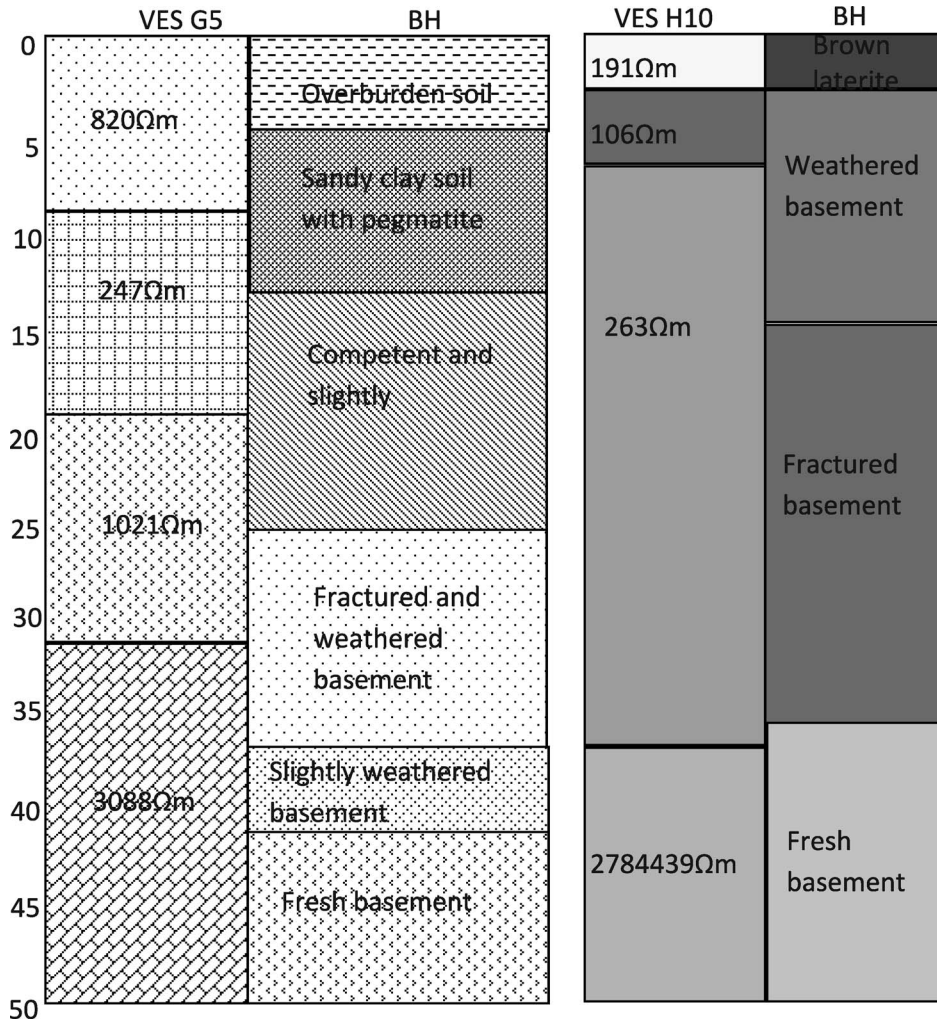


Figure 8—Corroboration of VES lithology with nearby borehole logs.

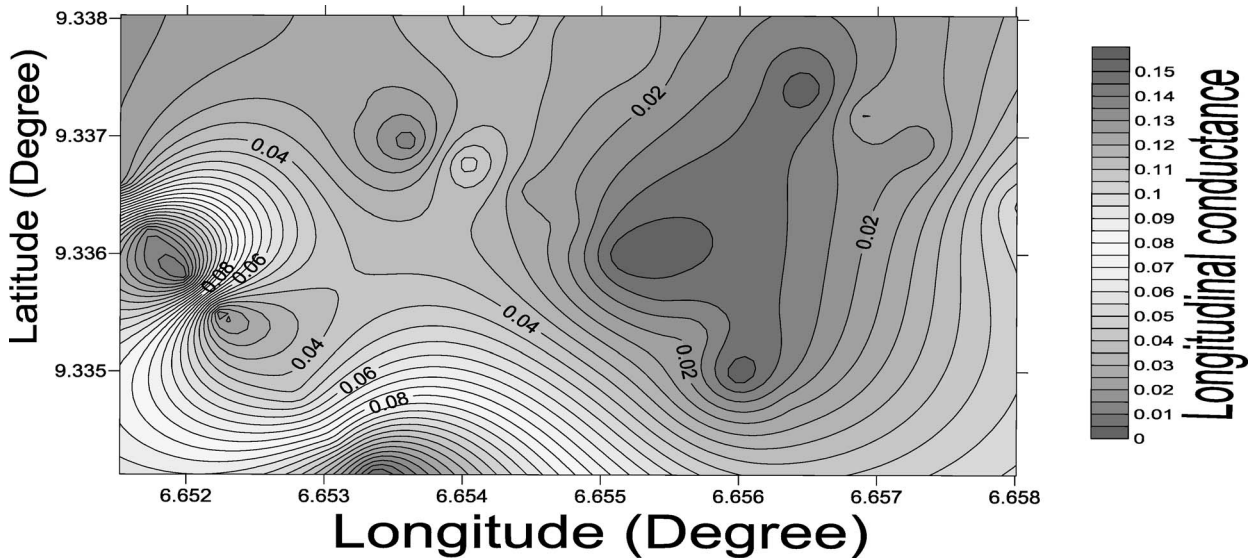


Figure 9—2-D contour map showing distribution of longitudinal conductance in the study area.

Table 2—Modified longitudinal conductance/protective capacity rating (Henriet, 1976; Oladapo et al., 2004).

Longitudinal conductance (mhos)	Protective capacity rating
>10	Excellent
5–10	Very good
0.7–4.9	Good
0.2–0.69	Moderate
0.1–0.19	Weak
<0.1	Poor

Conclusion

Northern Paiko was surveyed using VES to evaluate the groundwater potential and the aquifer protective capacity of the area. The analysis of the results revealed the subsurface lithologic units to include the topsoil, weathered layer, fractured layer, and fresh basement. The weathered layer constitutes the major aquifer unit in the area. The curve types were identified as H, HA, A, HK, KH, and K. The aquifer's resistivity and thickness values were used to compute the longitudinal conductance of the study area and hence generate the resistivity, thickness, and longitudinal conductance maps of the area. From the study, it was found that 3.3% of the study area falls within the high groundwater potential while 20 and 76.7% were medium and low, respectively. It can be said that the groundwater potential of the area is generally low. The study also revealed that 83.3% of the study area has poor aquifer protective capacity; as, such these areas are vulnerable to contamination from infiltration of leachate from dumpsites and sewage. The north-central part of the study area is mostly affected. The information from this study will be useful in prospecting and developing of borehole systems in the area.

Acknowledgments

The authors are grateful to Messrs. Victor Omonona and Osita Nnebedum of the Department of Geology, University of Nigeria, Nsukka, for their valuable contributions. They also thank immensely the reviewers for their thorough work and the executive editor of Water Environment Research for his meticulous and encouraging work.

Submitted for publication December 27, 2014; revised manuscript submitted August 2, 2015; accepted for publication September 16, 2015.

References

- Abiola, O.; Enikanselu, P. A.; Oladapo, M. I. (2009) Groundwater Potential and Aquifer Protective Capacity of Overburden Units in Ado-Ekiti, Southwestern Nigeria. *Int. J. Phys. Sci.*, **4**, 120-132.
- Adeleye, D. R. (1976) The Geology of the Middle Niger Basin. In *The Geology of Nigeria*, Kogbe, C. A., ed.; Elizabethan Publishing Company: Lagos, Nigeria; pp 283-287.
- Adeniji, A. E.; Obiora, D. N.; Omonona, O. V.; Ayuba, R. (2013) Geoelectrical Evaluation of Groundwater Potentials of Bwari Basement Area, Central Nigeria. *Int. J. Phys. Sci.*, **8**, 1350-1361.
- Ajibade, A. C. (1980) The Geology of the Country around Zungeru, Northwestern state of Nigeria. M.Sc. Thesis, University of Ibadan, Ibadan.
- Amadi, A. N.; Ameh, M. I.; Jisa, J. (2010) The Impact of Dumpsites on Groundwater Quality in Makurdi Meteropolis, Benue State. *Nat. Appl. Sci. J.*, **11**, 90-102.
- Amadi, A. N.; Olasehinde, P. I.; Okoye, N. O.; Momoh, O. I.; Dan-Hassan, M. A. (2012) Hydrogeophysical Exploration for Groundwater Potential in Kataregi, Northern-Central Nigeria. *Int. J. Sci. Res.*, **2**, 9-17.
- Bala, A. E.; Ike, E. C. (2001) The Aquifer of the Crystalline Basement Rocks in Gusau Area, Northeastern Nigeria. *J. Min. Geol.*, **37**, 177-184.
- Barker, R.; Rao, T. V.; Thangarajan, M. (2001) Delineation of Contaminant Zone through Electrical Imaging Technique. *Curr. Sci.*, **81**, 277-283.
- Clerk, L. (1985) Groundwater Abstraction from Basement Complex Areas of Africa. *J. Eng. Geol. London*, **18**, 25-34.
- Dan-Hassan, M. A. (2001) Determination of Geo-electric Sequences and Aquifer Units in Part of the Basement Complex of North-Central Nigeria. *Water Res. J. Niger. Assoc. Hydrogeol.*, **12**, 45-49.
- Du Preez, J. W.; Barber, W. (1965) The Distribution and Chemical Quality of Groundwater in Northern Nigeria. *Geol. Surv. Niger.*, **36**, 1-93.
- Egbai, J. C. (2011) A Combination of Electrical Resistivity and Seismic Refraction Surveys for Ground Water Exploration in Basement Region of Ifon, Ondo State, Nigeria. *Aust. J. Basic Appl. Sci.*, **5**, 1007-1016.
- George, N. J.; Akpan, A. E.; Obot, I. B. (2010) Resistivity Study of Shallow Aquifers in the Parts of Southern Ukanafun Local Government Area, Akwalbom State, Nigeria. *E-J. Chem.*, **7**, 693-700.
- Henriet, J. P. (1976) Direct Application of Dar Zarrowk Parameters in Groundwater Survey. *Geophys. Prospect.*, **24**, 344-353.
- Lashkaripour, G. R. (2003) An Investigation of Groundwater Condition by Geoelectrical Resistivity Method: A Case Study in Krin Aquifer Southeast Iran. *J. Spatial Hydrol.*, **3**, 1-5.
- Niwas, S.; Singhal, D. C. (1981) Estimation of Aquifer Transmissivity from Dar Zarrowk Parameters in Porous Media. *Hydrology*, **50**, 393-399.
- Oladapo, M. I.; Mohammed, M. Z.; Adeoye, O. O.; Adetola, O. O. (2004) Geoelectric Investigation of the Ondo State Housing Corporation Estate; Ijapo, Akure, Southwestern Nigeria. *J. Min. Geol.*, **40**, 41-48.
- Olasehinde, P. I.; Amadi, A. N. (2009) Assessment of Groundwater Vulnerability in Owerri and Its Environs, Southern Nigeria. *Niger. J. Technol. Res.*, **4**, 27-40.
- Olurunfemi, M. O.; Fasuyi, S. A. (1993) Aquifer Types and Geoelectrical/Hydrogeologic Characteristics of Central Basement Terrain of Nigeria. *J. Afr. Earth Sci.*, **16**, 309-317.
- Orellana, E.; Mooney, H. (1966) *Master Tables and Curves for VES over Layered Structures*; Interciencia: Madrid, Spain.
- Sharma, P. V. (1997) *Environmental and Engineering Geophysics*; Cambridge University Press: Cambridge, U.K.
- Singh, K. P. (2005) Nonlinear Estimation of Aquifer Parameters from Superficial Resistivity Measurements. *J. Hydrol. Earth Sys. Sci.*, **2**, 917-938.